Clim. Past Discuss., doi:10.5194/cp-2016-118, 2016
Manuscript under review for journal Clim. Past
Published: 1 December 2016

Climate of the Past Discussions
Open Access
EGU

Influence of North Pacific Decadal Variability on the Western Canadian Arctic over the past 700 years

François Lapointe[1,2], Pierre Francus[1,2], Scott F. Lamoureux[3], Mathias Vuille[4], Jean-Philippe Jenny[1,5], Raymond S. Bradley[6]

[1]Centre - Eau Terre Environnement, Institut National de la Recherche Scientifique Université du Québec, Québec, G1K 9A9, Canada

[2]GEOTOP Research Center, Montréal (Qc), H3C 3P8, Canada

[3]Department of Geography and Planning, Queen's University, Kingston, ON K7L 3N6, Canada

[4]Department of Atmospheric and Environmental Sciences, University at Albany, Albany, New York 12222, United States.

[5]Max-Planck-Institute for Biogeochemistry, 10, 07745 Jena, Germany

[6]Northeast Climate Science Center, and Climate System Research Center, Department of Geosciences, University of Massachusetts, Amherst, 01003, United States.

Correspondence to: François Lapointe (francois.lapointe@ete.inrs.ca)

Clim. Past Discuss., doi:10.5194/cp-2016-118, 2016
Manuscript under review for journal Clim. Past
Published: 1 December 2016

Climate of the Past Discussions
Open Access
EGU

Abstract

It is well established that the Arctic strongly influences global climate through positive feedback processes (Cohen et al., 2014), one of the most effective being the sea-ice – albedo feedback (Screen et al., 2010). Understanding the region's sensitivity to both internal and external forcings is a prerequisite to better forecast future global climate variations. Here, sedimentological evidence from an annually laminated (varved) record highlights that North Pacific climate variability has been a persistent regulator of the regional climate in the western Canadian Arctic. The varved record is negatively correlated with both the instrumental and reconstructed Pacific Decadal Oscillation (PDO) (D'arrigo et al., 2001; Gedalof et al., 2001; Macdonald et al., 2005; Mantua et al., 1997) throughout most of the last 700 years, suggesting drier conditions during high PDO phases, and vice-versa. This is in agreement with known regional teleconnections whereby the PDO is negatively and positively correlated with summer precipitation and mean sea level pressure, respectively. This pattern is also seen during the positive phase of the North Pacific Index (NPI) (Trenberth et al., 1994) in autumn. A reduced sea-ice cover during summer is observed in the region during PDO- (NPI+), as has been found during winter (Screen et al., 2016). Strongest during the autumn season, low-level southerly winds extend from the northernmost Pacific across the Bering Strait and can reach as far as the Western Canadian Arctic. These climate anomalies projecting onto the PDO- (NPI+) phase are key factors in enhancing evaporation and subsequent precipitation in this region. As projected sea-ice loss will contribute to enhanced future warming in the Arctic, future negative phases of the PDO (or NPI+) will likely act as amplifiers of this positive feedback (Screen et al., 2016).

Clim. Past Discuss., doi:10.5194/cp-2016-118, 2016
Manuscript under review for journal Clim. Past
Published: 1 December 2016

Climate of the Past Discussions
Open Access
EGU

1 Introduction

In the North Pacific region, the Pacific Decadal Oscillation (PDO) is the major mode of multi-decadal climate variability (Mantua et al., 1997). The PDO can be described as a long-lived El Niño/Southern Oscillation (ENSO)-like pattern of Pacific sea surface temperature (SST) variability (Zhang et al., 1997), or as a low-frequency residual of ENSO variability on multi-decadal time scales (Newman et al., 2003). During the warm (positive) PDO phase (PDO+), regions of southeast Alaska, the southwestern US and Mexico generally have increased winter precipitation, whereas drier conditions are observed in southern British Columbia and the Pacific Northwest US. During PDO- conditions are essentially reversed (Mantua and Hare 2002). To date, little is known, however, about the influence of the PDO on the climate of the Canadian Arctic. Indeed, the impacts of the PDO in this region have not been documented because of the lack of 1) reliable meteorological datasets, which generally don't extend prior to 1950, and 2) annually-resolved climate archives. Here, three different PDO reconstructions (D'arrigo et al., 2001; Gedalof et al., 2001; Macdonald et al., 2005) are compared with our varved record from Cape Bounty East Lake (Lapointe et al., 2012), located on Melville Island, and provide evidence that the PDO impacted this remote region at least over the last ~700 years. One-point correlation maps and observations at the nearest continuous weather station, Mould Bay, indicate that the PDO and the North Pacific Index (NPI), an index measuring the strength of the Aleutian Low (Trenberth et al., 1994), have been significant drivers of summer-autumn precipitation in the region.

Cape Bounty East Lake (hereafter CBEL, 5 m asl) is located on southern Melville Island in the Canadian Western High Arctic (74° 53' N, 109° 32'W). CBEL is a small (1.5 km^2) and relatively deep (32 m) monomictic freshwater lake. The lake has ice cover for 10-11 months of the year and has one primary river inflow. CBEL has been monitored since 2003 as part of comprehensive hydrological and limnological studies that revealed the nature of sediment delivery and deposition in this setting (Cockburn et al., 2008; Lamoureux et al., 2009; Lewis et al., 2011). Fluvial input to the lake occurs mainly during June and July during spring snowmelt and also due to major rainfall events generally later in the summer season

Clim. Past Discuss., doi:10.5194/cp-2016-118, 2016
Manuscript under review for journal Clim. Past
Published: 1 December 2016

(Dugan et al., 2009; Lapointe et al., 2012; Lewis et al., 2011). Previous studies (Cuven et al., 2011; Lapointe et al., 2012) demonstrated the presence of clastic varves in the lake and documented the past hydroclimatic variability using the physical and geochemical properties of the varve sequence. Finally, seismic profiles of the lake bottom revealed that the coring site used in Lapointe et al. (2012) and Cuven et al. (2011) was devoid of mass movement deposits, therefore ideal for paleoclimatic investigations (Normandeau et al. 2015).

2 Materials and methods

2.1 Observational climate data

To understand the recent relationship between the Western Canadian Arctic climate and the PDO, we calculated one-point correlation maps using the Pearson's correlation. These were prepared using the Climate Explorer tool that is managed by the Royal Netherlands Meteorological Institute (Trouet et al., 2013; Van Oldenborgh et al., 2005). Precipitation, sea-level pressure, temperature and sea-ice anomalies were obtained from the ERA-Interim reanalysis (Dee et al., 2011), a dataset that provides the most consistent observations of average temperature and precipitation in the Canadian Arctic (Lindsay et al., 2014; Rapaić et al., 2015). For zonal and meridional wind, we use the NCEP-NCAR (Kalnay et al., 1996) which cover the period 1950-2016. The PDO as defined in (1997) is derived as the leading principal component of monthly SST anomalies in the North Pacific Ocean, poleward of 20°N. A second PDO index, based on the Extended Reconstructed Sea Surface Temperature (ERSSTv4) dataset - a global monthly sea surface temperature dataset from the International Comprehensive Ocean-Atmosphere Dataset (ICOADS) (Huang et al., 2015) - was constructed by regressing the ERSSTv4 anomalies against the Mantua PDO index using the period of overlap, resulting in a PDO regression map for North Pacific ERSST anomalies. This index closely resembles the Mantua PDO index. The NPI is described as the area-weighted sea-level pressure over the region 30°N-65°N, 160°E-140°W (Trenberth et al., 1994). Finally the Arctic Oscillation Index, representing the leading Empirical Orthogonal Function (EOF) of monthly mean 1000 hPa geopotential height anomalies over 20°-90° N latitude (Thompson and Wallace 1998) was used. The Mould Bay weather station data, the closest to CBEL, was extracted from: http://climate.weather.gc.ca/historical_data/search_historic_data_e.html.

Clim. Past Discuss., doi:10.5194/cp-2016-118, 2016
Manuscript under review for journal Clim. Past
Published: 1 December 2016

2.2 Proxy data

Varve thickness and grain-size data (Lapointe et al., 2012), available from the NOAA paleoclimate database, were linearly detrended. A box-cox transformation was then used to stabilize variance in the time series (note that a log-transformation of the time series yielded similar results). The data were normalized to allow for a comparison with other time series. Three PDO reconstructions (D'arrigo et al., 2001; Gedalof et al., 2001; Macdonald et al., 2005) were used for comparison with our record. Spectral analyses were carried out using REDFIT (Schulz et al., 2002). Wavelet analyses were performed with the software R (Team, 2008) using the package biwavelet (Gouhier et al., 2012).

3 Results

3.1 Instrumental teleconnections

Several key climate indices demonstrate the present-day influence of the PDO on the Western Canadian Arctic. The correlation between the PDO index (Mantua et al., 1997) based on ERSSTv4 (Huang et al., 2015) and sea-ice cover (Dee et al., 2011) is positive during summer and autumn over the region (Figures 1a, S1). An anomalous surface high-pressure system develops in the vicinity of southern Melville Island from July to September (JAS) (Figure 1b) during positive PDO phases (PDO+). The PDO index is also inversely correlated with summer rainfall from the nearest continuous weather station, Mould Bay (Figure 1c), implying drier (wetter) conditions during the positive (negative) phase of the PDO ($r = -0.47$, $p < 0.0001$). This suggests that PDO-related atmospheric circulation anomalies significantly affect the climate of this region (Fig. 1).

Another important teleconnection is revealed in the spatial correlation between PDO and mean sea level pressure (mslp) during winter (Fig. 1d). The mid-to high-latitude manifestation of the PDO includes a wave train that is characterized by a deepening of the Aleutian Low and a high-pressure system to the northeast over the Canadian Arctic during PDO+, somewhat reminiscent of the Pacific - North America pattern PNA (Wallace and Gutzler, 1981), and most prominent during

Clim. Past Discuss., doi:10.5194/cp-2016-118, 2016
Manuscript under review for journal Clim. Past
Published: 1 December 2016

the positive phase of ENSO. Melville Island is located at the core of this teleconnection wave train, and is ideally located to sample extremes of the PDO as they are expressed as significant departures of mslp during each phase (Fig.1d). The existence of a persistent anomalous high-pressure system over this area during the PDO+ is indicative of drier than average conditions in the region, while negative mslp anomalies during the negative PDO phase (PDO-) likely reflect the more frequent passage of low-pressure systems and the increased likelihood of precipitation (Fig. 1c).

The Western Canadian Arctic is also strongly influenced by the North Pacific Index (NPI) during September-November (SON) (Fig. 2). The NPI is a more direct measure of the strength of the Aleutian Low (Trenberth et al., 1994) and has been shown to be part of the PDO North Pacific teleconnection (Schneider et al., 2005). A weakened Aleutian Low (increased mslp) is seen in the Pacific during times of positive NPI (NPI+), as is the case during PDO-. Meanwhile, an anomalous low-pressure system is observed over the Western Canadian Arctic (Fig. 2a), consistent with an increased likelihood of precipitation (Fig. 2b). This is confirmed by the correlation between snow depth recorded at Mould Bay and the NPI (Fig. 2c).

3.2 Comparison with instrumental and paleo-PDO records

The sedimentary varve record gives support to these instrumental climate observations. Annual coarse grain-size (98^{th} percentile) (Lapointe et al., 2012) is negatively correlated with the instrumental PDO (Mantua et al., 1997) during the last 100 years ($r = -0.31$, $p = 0.001$; and $r = -0.84$ using a 10-year low-pass filter, Fig. 3), suggesting thicker varves (deposits) during PDO-. A similar correlation is found between instrumental NPI (Trenberth and Hurrell 1994) and coarse grain-size at CBEL (Fig. S2 : $r = 0.30$, $p = 0.003$).

For earlier periods, we use the time interval 1300-1900 to compare our CBEL varve thickness (VT) record to paleo-PDOs as only one erosive bed is seen in the sedimentary record during this period (Text 1, Fig. S4). The three reconstructed PDOs (MacDonald and Case 2005, Gedalof and Smith 2001, DArrigo et al. 2001) show periods of high coherency, but there are periods of low consistency between them (Fig. 4a-c), as reported in the literature (Kipfmueller et al., 2012; Wise, 2015). To better explain the variance in the paleo-PDO time series, a principal component analysis (PCA) was performed on the three PDO-records. The PC1 (Fig. 4d) explains 51% of the variability and its highest correlation with VT is achieved with an

Clim. Past Discuss., doi:10.5194/cp-2016-118, 2016
Manuscript under review for journal Clim. Past
Published: 1 December 2016

18 year lag (Fig. S3: r = -0.29, p < E-5). Given the present-day teleconnection (Figs. 1-2) and the overall co-variability between the instrumental PDO and our record (Fig. 3), this lag is likely due to intrinsic errors of varve chronologies (Ojala et al., 2012) rather than a mechanistic phase shift (Text S1). When applying a 5-year running-mean on the series the co-variability is striking (r = -0.48), especially from 1750-1900 (r = -0.68). From 1600-1900, annual correlation between Gedalof and Smith (2001) and our record is significant (r = -0.21, p < 0.001). When a 5-year running mean is applied on the series, the coherence between both records is much stronger (Fig. 4b: r = -0.39). This is also the case when comparing our CBEL VT record to the D'Arrigo et al. (2001) PDO (Fig. 4c, annual correlation: r = -0.25, p < 0.001; 5 yr-running mean: r = -0.29). The correlation of our record to the PDO from MacDonald and Case for the period 1446-1900 is also significant (annual correlation: r = -0.24, p < E-7, 5 year-running mean: r = -0.39). For the period encompassing 1300-1446 CE, we note that the records are significantly correlated with a 28 year-lag. This broader lag is likely related to erosion produced by a high-energy event (second largest layer of the record) dated at ~1446 CE (Fig. S4). When shifting our record back by 28 years, a high co-variability exists between both records (Figs. 4a, S5). The overall annual correlation with the MacDonald and Case (2005) index is slightly improved during the pre-industrial interval 1300-1845 CE (Figs. 4a: annual correlation: r = -0.27, p < E-10, r = -0.43 (5-year running-mean) and -0.69 (25-year low-pass filter, Fig. S5).

3.3 Spectral content of the 244-2000 CE period

To further support the link between our site and the PDO (NPI), spectral analysis of the entire VT record for the 244-2000 CE period found significant (> 99% confidence level (CL); Fig. 5a) spectral peaks at ~19-26 and at 62 years that are consistent with those found in the high-frequency (19-25 year) and also the lower frequency range (50-70 year) of the PDO (Chao et al., 2000; Latif et al., 1996; Mantua et al., 2002; Minobe, 1997; Tourre et al., 2005). The 2-4 year-cycle in the VT could be linked to ENSO, which is characterized by high-frequency variability of 2-8 years (Deser et al., 2010). Many significant sub-decadal periodicities at ~2-8 years are observed (Fig. 5b). These periodicities are particularly pronounced from 1450 to 2000 CE and 800 to 1200 CE. Over the last millennium, the 50-70 year oscillation has been persistent at Cape Bounty from ~1000 to 1550 CE and from ~1700 CE until recently (Fig. 5b). This is somewhat different from the PDO reconstruction from tree-rings (Macdonald et al., 2005) in which the wavelet spectrum displays a persistent power band

Clim. Past Discuss., doi:10.5194/cp-2016-118, 2016
Manuscript under review for journal Clim. Past
Published: 1 December 2016

covering only the periods ~1350-1500 CE and 1800 CE until recently. Similar to MacDonald and Case (2005), CBEL reveals a weaker or disappearing multi-decadal variability during the 17th century and the early part of the 18th century. However, in contrast to MacDonald and Case (2005), significant power located at 2-8 years remains relatively constant during most of the past millennium in CBEL and is particularly strong between ~850-1250 CE (Medieval Climate Anomaly, MCA), ~1450-1750 CE (coldest interval of the LIA), and recently (Fig. 5b). A ~60 year periodicity is also clearly discernible during 600-800 CE, a period also characterized by strong decadal and sub-decadal (2-7 year) cycles. Altogether, these relationships point toward a significant influence of the PDO on the Western Canadian Arctic.

4 Possible mechanisms linking our record to the PDO

As the Western Canadian Arctic is characterized by lower pressure system anomalies when the Aleutian Low is in a weakened state (increased SLP, NPI+, Fig. 2), it is plausible that the prevailing winds reaching our region originate from the Northern Pacific. Indeed, a negative correlation between meridional windstress and the NPI during SON over the northernmost part of the Pacific and extending into the Western Canadian Arctic (Fig. 6a) indicates prevailing northerly wind anomalies during the positive phase of the NPI. It has been shown that PDO and Arctic Oscillation (AO) when both are in a positive increase summer precipitation in regions of Alaska (L'Heureux et al., 2005). The correlation between the AO and the meridional windstress anomalies (Fig. 6b) yields very similar pattern as the NPI (Fig. 6a), albeit slightly less significant results. This is not too surprising, since these two climate indices are significantly correlated during SON (1900-2015: $r = 0.45$, $p < 0.0001$). Hence the two modes, during AO+ and NPI+, might constructively interfere to strengthen northerly winds over the Arctic, converging with southerly moisture-laden winds from the North Pacific over the Western Canadian Arctic, thereby favoring precipitation in the region during autumn.

We note that these meridional wind anomalies appear to persist during the cold season (Fig. S8), although they are not as pronounced over the Western Canadian Arctic as in September-November (Fig. 6a). This is consistent with annual surface wind stress differences between PDO phases over the North Pacific (Zhang et al., 2015) during the 20th century (Fig. 7). Indeed, sustained southerly wind anomalies are observed in the northernmost part of the Pacific during PDO- (induced by

Clim. Past Discuss., doi:10.5194/cp-2016-118, 2016
Manuscript under review for journal Clim. Past
Published: 1 December 2016

a weakened Aleutian Low, i.e. NPI+), north of the Kuroshio-Oyashio Extension, where warm SST anomalies are observed (Screen et al., 2016; Zhang et al., 2015) (Fig. 7). These southerly winds extend from the northernmost Pacific (north of the weakened Aleutian Low) across the Bering Strait and can reach as far as the Western Canadian Arctic, increasing heat and moisture transport into the latter region (Screen et al., 2016). Meanwhile, strong westerly winds dominate over the eastern Siberian shelf and converge with the southerly flow from the Pacific over the Western High Arctic during PDO- (Kwon et al., 2007; Screen et al., 2016; Zhang et al., 2015) (Fig. 7). Thus, the PDO phase has been shown to clearly influence the winter-mean atmospheric circulation in the North Pacific while its influence also extends into the Arctic (Screen and Francis 2016). Our analysis suggests that this PDO (NPI) influence might also be impacting regional climate during autumn.

Warmer summer temperatures during PDO- are also observed in large areas of the Arctic (Fig. S9a). This is most apparent in the Western Canadian Arctic during NPI+ (Fig. S9b). It is known that PDO- (and NPI+) lead to lower tropospheric Arctic warming and sea-ice loss (Screen et al., 2016). The combination of reduced sea-ice extent (Figs. 1, S1) and warmer surface temperature during PDO- (NPI+) (Fig. S9) likely allows for more evaporation to occur, while anomalous surface winds (Figs. 6,7) are increasing moisture convergence in the region, thereby enhancing precipitation during times of PDO- (NPI+) (Figs. 1c, 2b,c). Analyses by Francis et al. (2009) have shown that the Aleutian Low tends to be weaker following summers of reduced sea ice cover. A comparison between our record and instrumental sea-ice extent since 1979 (Cavalieri et al., 1996) (Fig. S10: $r = -0.52$, $p = 0.01$) suggests increased precipitation during times of low sea-ice extent. Winds during periods of a weakened Aleutian Low (Figs. 6,7) and reduced sea-ice extent in the region, as seen during PDO- (Fig. 1a), would likely be more effective at transporting moisture across the Western Canadian Arctic (Fig. 2b). More importantly, Arctic sea-ice extent reached unprecedented low values in the latter half of the 20th century compared to the last 1,450 years (Kinnard et al., 2011). This trend is similar to the coarse grain-size at CBEL, which increased substantially and reached unprecedented levels in the 20th century compared to the last 1750 years (Lapointe et al. 2012). All of these elements point to a causal mechanism, linking the NPI (PDO), sea-ice and precipitation in the Western Canadian Arctic.

Clim. Past Discuss., doi:10.5194/cp-2016-118, 2016
Manuscript under review for journal Clim. Past
Published: 1 December 2016

5 Conclusion

This study suggests a significant influence of the PDO (NPI) on the climate of the Western Canadian Arctic, a region where instrumental data coverage is very sparse and the duration of available records is short. Spatial correlations using both instrumental and reanalysis data indicate a strong atmospheric teleconnection, likely responsible for the increase of precipitation during PDO- (NPI+). These results indicate the importance of large-scale teleconnections for Arctic climate and in particular, for precipitation variations in the Canadian High Arctic. The PDO – Western Canadian Arctic relationship has persisted at least for the past ~700 years as revealed by the strong coherence between the CBEL varve record and multiple PDO reconstructions, suggesting some potential for decadal-scale climate prediction. Future warming is projected to further decrease mslp and increase precipitation in Arctic regions (Screen et al., 2015). As the sea-ice extent will continue to decrease in the following decades, precipitation might increase in the Western Canadian Arctic, especially under a warmer Arctic; a pattern which will likely be amplified during the PDO- (NPI+) (Screen and Francis 2016).

References

Cavalieri, D., Parkinson, C., Gloersen, P., and Zwally, H., 1996. Sea ice concentrations from Nimbus-7 SMMR and DMSP SSM/I-SSMIS passive microwave data (updated 2008). NASA Distributed Active Archive Center, National Snow and Ice Data Center, Boulder, CO, available at: http://nsidc. org/data/nsidc-0051.html. Last access September 2016.

Chao, Y., Ghil, M. and McWilliams., J-C.: Pacific interdecadal variability in this century's sea surface temperatures, Geophys. Res. Lett., 27**,** 2261-2264, doi: 10.1029/1999GL011324, 2000.

Cockburn, J. M. H. and Lamoureux, S.F.: Hydroclimate controls over seasonal sediment yield in two adjacent High Arctic watersheds, Hydrol Process., 22**,** 2013-2027, doi: 10.1002/hyp.6798, 2008.

Cohen, J., Screen, JA., Furtado, J.C., Barlow, M., Whittleston, D., Coumou, D., Francis, J., Dethloff, K., Entekhabi, D. and Overland, J.: Recent Arctic amplification and extreme mid-latitude weather, Nature Geosci., 7**,** 627-637, doi:10.1038/ngeo2234, 2014.

Cuven, S., Francus, P. and Lamoureux SF.: Mid to Late Holocene hydroclimatic and geochemical records from the varved sediments of East Lake, Cape Bounty, Canadian High Arctic, Quatern. Sci. Rev., 30 2651-2665, 2011.

D'Arrigo, R., Villalba, R. and Wiles, G.: Tree-ring estimates of Pacific decadal climate variability, Clim. Dynam., 18**,** 219-224, doi: 10.1007/s003820100177, 2001.

Clim. Past Discuss., doi:10.5194/cp-2016-118, 2016
Manuscript under review for journal Clim. Past
Published: 1 December 2016

D'Arrigo, R. D., Cook, ER., Mann, ME. and Jacoby GC., Tree-ring reconstructions of temperature and sea-level pressure variability associated with the warm season Arctic Oscillation since AD 1650, Geophys. Res. Lett., 30, doi: 10.1029/2003GL017250, 2003.

Dee, D., S. Uppala, A., Simmons, P., Berrisford, P., Poli, S., Kobayashi, U., Andrae, M., Balmaseda, G., Balsamo and Bauer P.: The ERA-Interim reanalysis: Configuration and performance of the data assimilation system, Q. J. R. Meteorol. Soc., 137**,** 553-597, 10.1002/qj.828, 2011.

Deser, C., Alexander, M.A., Xie, S.-P. and Phillips, A.S.: Sea surface temperature variability: Patterns and mechanisms, Ann. Rev. Mar. Sci., 2, 115-143, 2010.

Dugan, H.A., Lamoureux, S.F., Lafrenière, M.J. and Lewis, T.: Hydrological and sediment yield response to summer rainfall in a small high Arctic watershed, Hydrol. Process., 23, 1514-1526, doi:10.1002/hyp.7285 2009.

Gedalof, Z. and Smith, D.J.: Interdecadal climate variability and regime-scale shifts in Pacific North America, Geophys. Res. Lett., 28**,** 1515-1518, doi: 10.1029/2000GL011779, 2001.

Gouhier, T. and Grinsted, A.: biwavelet: Conduct univariate and bivariate wavelet analyses. R package version 0.13, Available at : https://cran.r project.org/web/packages/biwavelet/biwavelet.pdf, Acessed February 2016.

Huang, B., Banzon, V. F., Freeman, E., Lawrimore, J., Liu, W., Peterson, T.C., Smith, T.M., Thorne, P.W., Woodruff, S.D. and Zhang, H.-M.: Extended reconstructed sea surface temperature version 4 (ERSST. v4), Part I: upgrades and intercomparisons, J. Climate, 28**,** 911-930, 2015.

Kalnay, E., Kanamitsu, M., Kistler, R., Collins, W., Deaven, D., Gandin, L., Iredell, M., Saha, S., White, G. and Woollen, J.: The NCEP/NCAR 40-year reanalysis project. B. Am. Meteorol. Soc., 77**,** 437-471, 1996.

Kinnard, C., Zdanowicz, C.M., Fisher, D.A., Isaksson, E., de Vernal, A. and Thompson, L.G.: Reconstructed changes in Arctic sea ice over the past 1,450 years, Nature, 479**,** 509-512, doi:10.1038/nature10581, 2011.

Kipfmueller, K. F., Larson, E.R. and St George S.: Does proxy uncertainty affect the relations inferred between the Pacific Decadal Oscillation and wildfire activity in the western United States?, Geophys. Res. Lett. 39, doi: 10.1029/2011GL050645, 2012.

Kwon, Y.-O. and Deser, C.: North Pacific decadal variability in the community climate system model version 2, J. Climate, 20**,** 2416-2433, 2007.

Lamoureux, S. F. and Lafrenière, M.J.: Fluvial impact of extensive active layer detachments, Cape Bounty, Melville Island, Canada, Arct. Antarct. Alp. Res., 41**,** 59-68, 2009.

L'Heureux, M.L., Mann, M.E., Cook, B.I., Gleason, B.E. and Vose, R.S.: Atmospheric circulation influences on seasonal precipitation patterns in Alaska during the latter 20th century, 109(D6), J. Geophys. Res.: Atmos., doi: 10.1029/2003JD003845, 2004.

Clim. Past Discuss., doi:10.5194/cp-2016-118, 2016
Manuscript under review for journal Clim. Past
Published: 1 December 2016

Lapointe, F., Francus, P., Lamoureux, SF., Saïd, M. and Cuven, S.: 1750 years of large rainfall events inferred from particle size at East Lake, Cape Bounty, Melville Island, Canada, J. Paleolimnol., 48, 159-173, doi: 10.1007/s10933-012-9611-8, 2012.

Latif, M. and Barnett, T.P.: Decadal climate variability over the North Pacific and North America: Dynamics and predictability, J. Climate, 9**,** 2407-2423, 1996.

Lewis, T., Lafrenière M.J. and Lamoureux, S.F.: Hydrochemical and sedimentary responses of paired High Arctic watersheds to unusual climate and permafrost disturbance, Cape Bounty, Melville Island, Canada, Hydrol. Process., 26**,** 2003-2018, doi: 10.1002/hyp.8335, 2012.

Lindsay, R., Wensnahan, M., Schweiger, A. and Zhang, J.:Evaluation of seven different atmospheric reanalysis products in the Arctic*, J. Climate, 27**,** 2588-2606, 2014.

MacDonald, G. M. and Case, R.A.: Variations in the Pacific Decadal Oscillation over the past millennium, Geophys. Res. Lett., 32, 10.1029/2005GL022478, 2005.

Mantua, N. J. and Hare S.R.: The Pacific decadal oscillation, J. Oceanogr., 58**,** 35-44, 2002.

Mantua, N. J., Hare, S.R., Zhang, Y., Wallace, J.M. and Francis, R.C.: A Pacific interdecadal climate oscillation with impacts on salmon production, B. Am. Meteorol. Soc., 78**,** 1069-1079, 1997.

Minobe, S.: A 50-70 year climatic oscillation over the North Pacific and North America, Geophys. Res. Lett., 24**,** 683-686, doi: 10.1029/97GL00504, 1997.

Newman, M., Compo, G.P. and Alexander, M.A.: ENSO-forced variability of the Pacific decadal oscillation, J. Climate, 16**,** 3853-3857, 2003.

Normandeau A., Joyal G., Lajeunesse P., Francus P., Lamoureux SF. and Lapointe F.: Late-Holocene Mass Movements in High Arctic East Lake, Melville Island (Western Canadian Arctic Archipelago). Submarine Mass Movements and their Consequences: Springer; 2016. p. 311-20.

Ojala, A., Francus, P., Zolitschka, B., Besonen M., and Lamoureux, SF.: Characteristics of sedimentary varve chronologies–a review, Quatern. Sci. Rev., 43**,** 45-60, 2012.

Porter, T. J., Pisaric, M.F., Field, R.D., Kokelj, S.V., Edwards, T.W., Healy, R. and LeGrande, A.: Spring-summer temperatures since AD 1780 reconstructed from stable oxygen isotope ratios in white spruce tree-rings from the Mackenzie Delta, northwestern Canada, Clim. Dynam., 42**,** 771-785, doi: 10.1007/s00382-013-1674-3, 2014.

Rapaić, M., Brown, R., Markovic, M. and Chaumont, D.: An evaluation of temperature and precipitation surface-based and reanalysis datasets for the Canadian Arctic, 1950–2010, Atmos.-Ocean, 53**,** 283-303, 2015.

Schneider, N. and Cornuelle, B.D.: The forcing of the pacific decadal oscillation*, J. Climate, 18**,** 4355-4373, 2005.

Schulz, M. and Mudelsee, M.: REDFIT: estimating red-noise spectra directly from unevenly spaced paleoclimatic time series. Comput. Geosci., 28**,** 421-426, 2002.

Screen, J. A., Deser, C. and Sun, L.: Projected changes in regional climate extremes arising from Arctic sea ice loss. Environ. Res. Lett., 10**,** 084006, 2015.

Screen, J. A. and Francis, J.A.: Contribution of sea-ice loss to Arctic amplification regulated by Pacific Ocean decadal variability, Nature Clim. Change, 1758-6798, doi:10.1038/nclimate3011, 2016.

Screen, J. A. and Simmonds, I.: The central role of diminishing sea ice in recent Arctic temperature amplification, Nature, 464**,** 1334-1337, doi:10.1038/nature09051, 2010.

Team, R. D. C. (2008) R: A language and environment for statistical computing. R Foundation for Statistical Computing, Vienna, Austria. Available at: URL http://www.r-project.org/, Accessed February 2015.

Thompson, D. W. and Wallace, J.M.: The Arctic Oscillation signature in the wintertime geopotential height and temperature fields, Geophys. Res. Lett., 25**,** 1297-1300, doi:10.1029/98GL00950, 1998.

Tourre, Y. M., Cibot, C., Terray, L., White, W.B. and Dewitte B.: Quasi-decadal and inter-decadal climate fluctuations in the Pacific Ocean from a CGCM. Geophys. Res. Lett., 32, doi: 10.1029/2004GL022087, 2005.

Trenberth, K. E. and Hurrell, J.W.: Decadal atmosphere-ocean variations in the Pacific. Clim. Dynam.,9**,** 303-319, doi:10.1007/BF00204745, 1994.

Trouet, V. and Van Oldenborgh, G.J.: KNMI Climate Explorer: a web-based research tool for high-resolution paleoclimatology, Tree-Ring Res., 69**,** 3-13, 2013.

Van Oldenborgh, G. J. and Burgers, G.: Searching for decadal variations in ENSO precipitation teleconnections, Geophys. Res. Lett., 32, doi:10.1029/2005GL023110, 2005.

Wallace, J.M., and Gutzler, D.S.: Teleconnections in the geopotential height field during the northern hemisphere winter, Mon. Wea. Rev., 109, 784–812, 1981.

Wise, E. K.:Tropical Pacific and Northern Hemisphere influences on the coherence of Pacific Decadal Oscillation reconstruction, Int. J. Climatol., 35**,** 154-160, doi: 10.1002/joc.3966, 2015.

Zhang, L. and Delworth, T.L.: Analysis of the characteristics and mechanisms of the Pacific Decadal Oscillation in a suite of coupled models from the Geophysical Fluid Dynamics Laboratory, J. Climate , 28**,** 7678-7701, 2015.

Zhang, Y., Wallace, J.M. and Battisti, D.S.: ENSO-like interdecadal variability: 1900-93, J. Climate,10**,** 1004-1020, 1997.

Clim. Past Discuss., doi:10.5194/cp-2016-118, 2016
Manuscript under review for journal Clim. Past
Published: 1 December 2016

Climate of the Past Discussions
Open Access
EGU

Acknowledgement

We wish to thank the Polar Continental Shelf Program for their field logistic support and NSERC grants to PF and SFL. FL is grateful to grants provided by the FRQNT and the W. Garfield Weston Foundation. We thank Geert Jan van Oldenborgh for advice with the use of the KNMI database. We also thank James Screen for constructive advice, and Byron Steinman and Ze'ev Gedalof who provided information on PDOs datasets. Paleo-data used in this study can be found on the NOAA server https://www.ncdc.noaa.gov/data-access/paleoclimatology-data/datasets

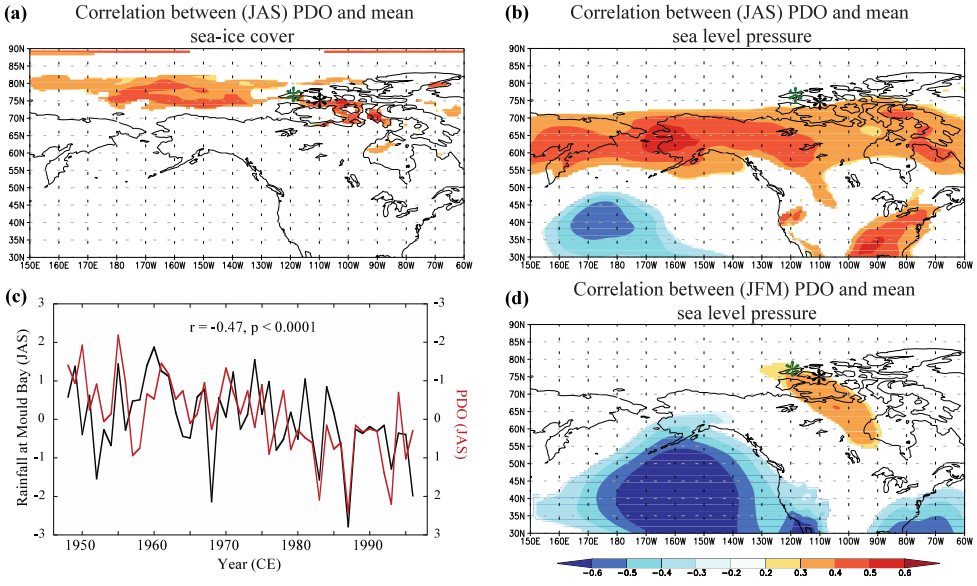

Figure 1. PDO modulation of Western Canadian Arctic climate. (a), Correlation between PDO (Huang et al., 2015) and sea-ice anomalies from ERA-Interim (Dee et al., 2011) for July-September during 1979-2016. (b), as in a) but for mean sea level pressure from ERA-Interim (Dee et al., 2011). (c), Correlation between rainfall at Mould Bay and PDO during July-September. (d), as in b) but for January-March (JFM). Black and green asterisks denote Cape Bounty and Mould Bay weather station, respectively. Note that Mould Bay weather station stopped operating in 1996.

Clim. Past Discuss., doi:10.5194/cp-2016-118, 2016
Manuscript under review for journal Clim. Past
Published: 1 December 2016

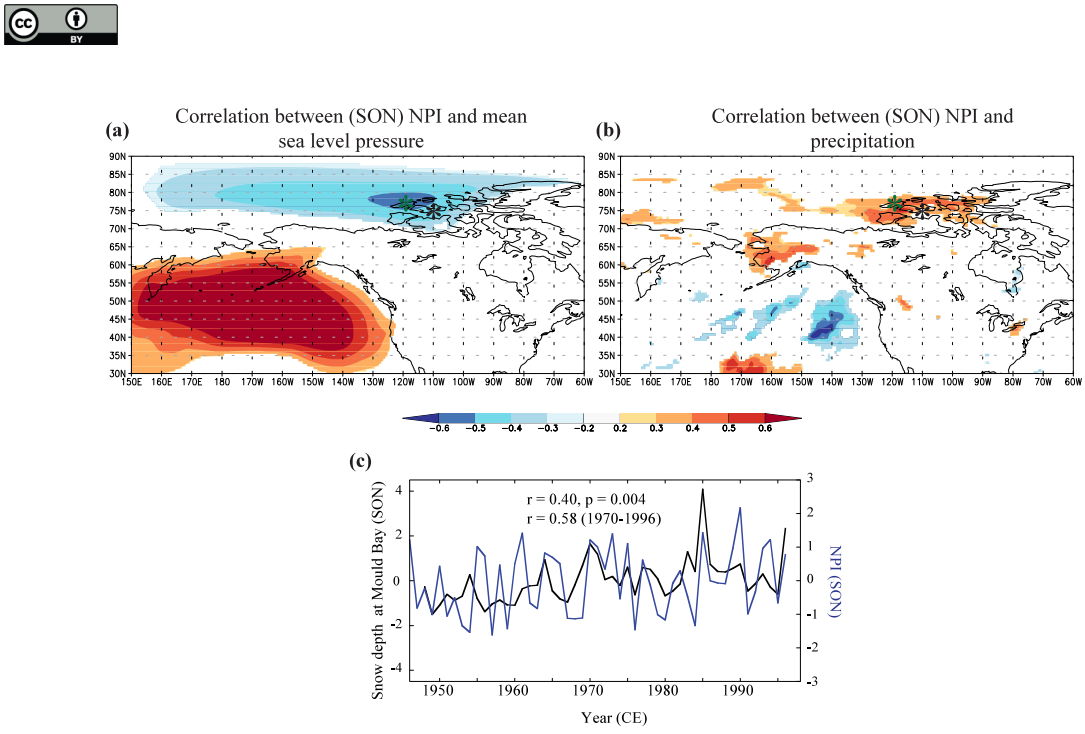

Figure 2. North Pacific Index (NPI) and precipitation during September-November. (a), Correlation between NPI (Trenberth et al., 1994) and mean sea level pressure from 1979-2015. (b), Same as (a), but for precipitation anomalies (Dee et al., 2011) correlated with NPI index. Black and green asterisks denote Cape Bounty and Mould Bay weather station, respectively. (c) Correlation between Mould Bay snow depth and NPI during September-November (Trenberth et al., 1994). Note that Mould Bay weather station stopped operating in 1996 CE.

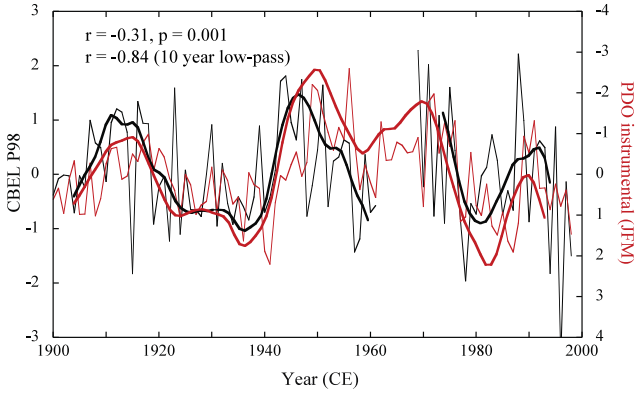

Figure 3. Instrumental PDO (NOAA) and compared with grain size at Cape Bounty East Lake from 1900-2000. (best correlation is achieved when CBEL lags PDO by 2 years). Bold lines are 10-year low-pass filtered. Seven years were eroded by a large turbidite dated to 1971 CE (Lapointe et al. 2012).

Clim. Past Discuss., doi:10.5194/cp-2016-118, 2016
Manuscript under review for journal Clim. Past
Published: 1 December 2016

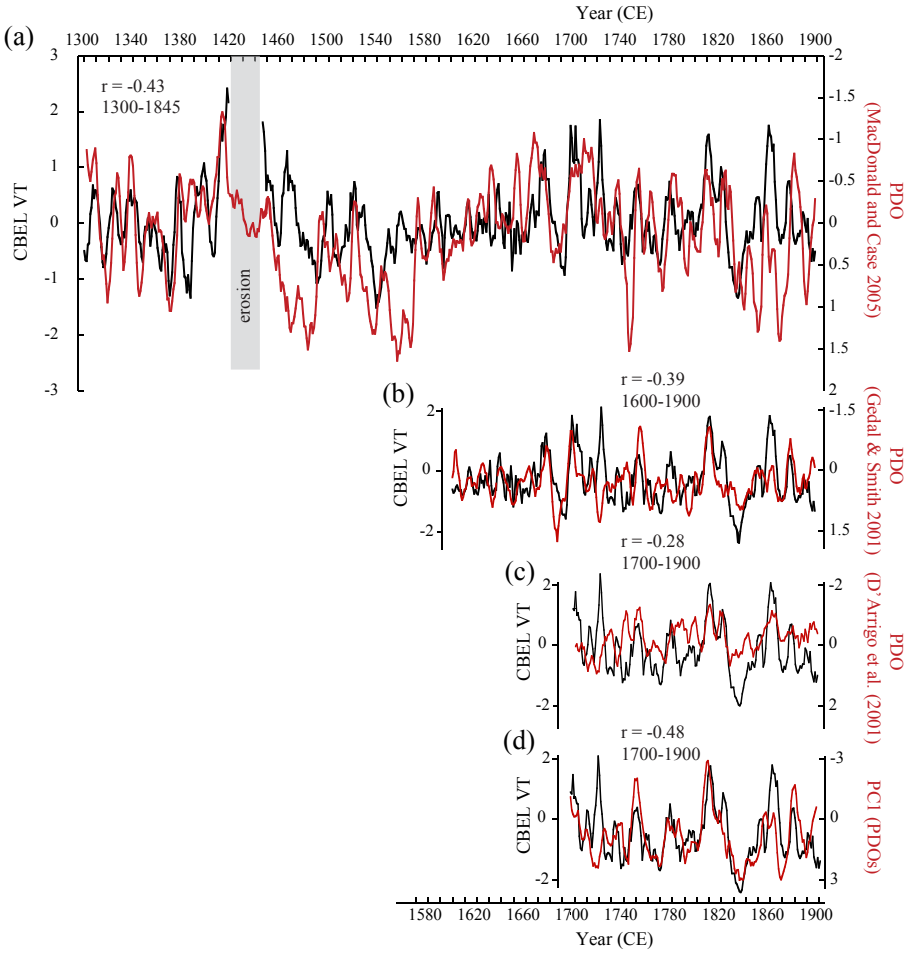

Figure 4. a), Comparison between normalized Cape Bounty East Lake varve thickness and normalized PDO from MacDonald and Case (2005) (VT is shifted 18 years earlier). b), Same as A) but for the PDO from Gedalof and Smith (2001). c), Same as a) and b) but using the PDO from D'Arrigo et al. (2001). d), Same as a), b) and c) but using the PC1 extracted from PCA analysis of the three PDOs. Time series are filtered by a 5-year running-mean.

Clim. Past Discuss., doi:10.5194/cp-2016-118, 2016
Manuscript under review for journal Clim. Past
Published: 1 December 2016

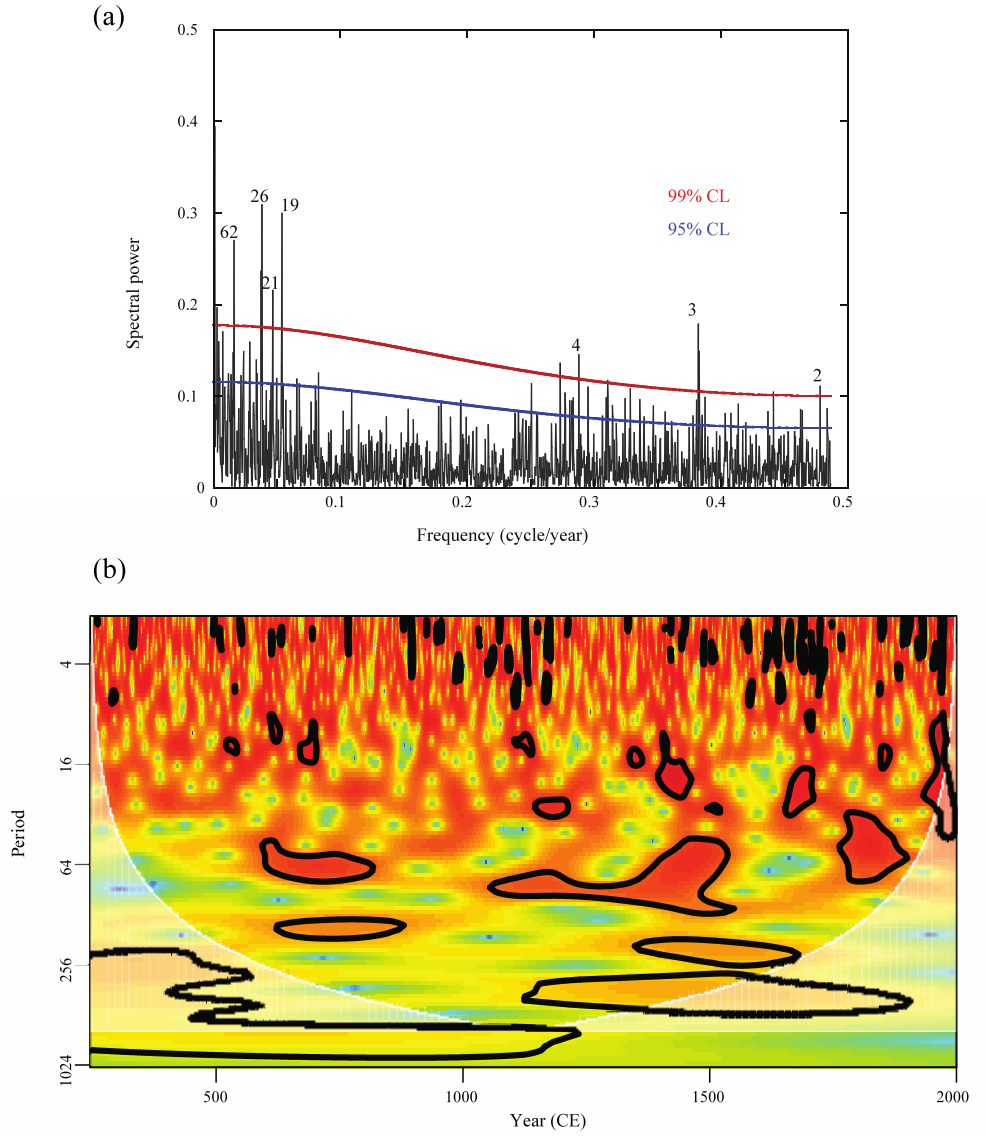

Figure 5. a), Spectral analysis of the varve thickness series. After Schulz and Mudelsee (Schulz et al., 2002). b), Wavelet analysis: black boundaries show the 95% confidence level based on a red noise process. White shading represents the cone of influence where edge effects might be important.

Clim. Past Discuss., doi:10.5194/cp-2016-118, 2016
Manuscript under review for journal Clim. Past
Published: 1 December 2016

Climate of the Past Discussions
Open Access
EGU

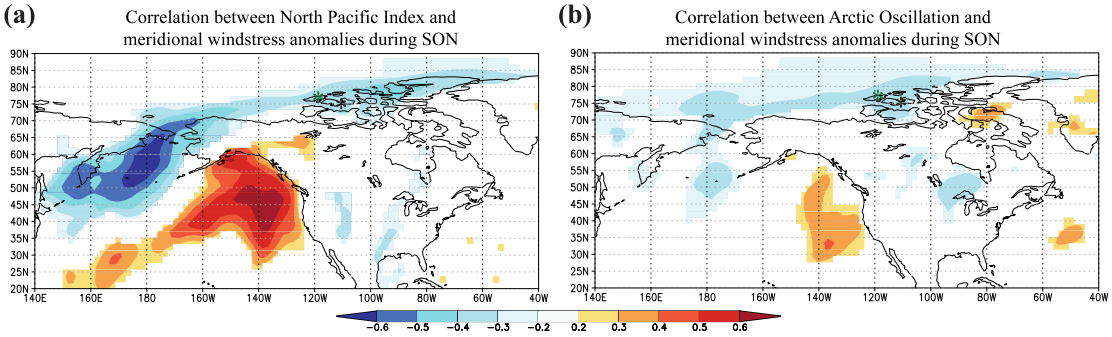

Figure 6. a), Correlation between NPI (Trenberth et al., 1994) and meridional windstress anomalies from 1950-2015. b), Same as a), but for correlation with Arctic Oscillation index (derived from NCEP/CPC). Note that the Era-Interim dataset yields similar result (not shown). Black and green asterisks denote Cape Bounty and Mould Bay weather station, respectively.

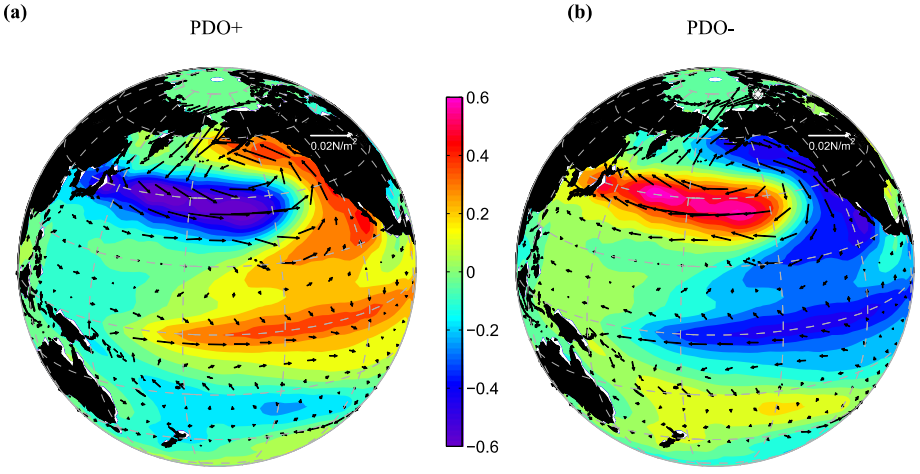

Figure 7. PDO modulation of winds and sea surface temperature in the Pacific. From Zhang and Delworth (Zhang et al., 2015). Regression of SST (°C) and surface wind stress (N m^2) against the PDO index. Note the northward direction of the wind stress in the central northern part of the Pacific during the negative phase of the PDO (b). Winds from the Siberian shelf have an eastward direction and reach Melville Island during negative PDO. Reproduced with permission from the American Meteorological Society (AMS).